Univariate polynomial equation providing on-lattice higher-order models of thermal lattice Boltzmann theory

Jae Wan Shim*
KIST and University of Science and Technology, 136-791, Seoul, Korea
(Received 22 February 2011; revised manuscript received 19 June 2012; published 29 January 2013)

A univariate polynomial equation is presented. It provides on-lattice higher-order models of the thermal lattice Boltzmann equation. The models can be accurate up to any required level and can be applied to regular lattices, which allow efficient and accurate approximate solutions of the Boltzmann equation. We derive models approaching the complete Galilean invariant and providing accuracy of the fourth-order moment and beyond. We simulate one-dimensional thermal shock tube problems to illustrate the accuracy of our models. Moreover, we show the remarkably enhanced stability obtained by our models and our discretized equilibrium distributions.

DOI: 10.1103/PhysRevE.87.013312 PACS number(s): 47.11.−j, 05.20.Dd

I. INTRODUCTION

The kinetic theory of gases constitutes the statistical theory of the dynamics of mechanical systems based on a simplified molecular description of a gas, from which macroscopic physical properties of the gas can be derived by using a velocity distribution function which describes how molecular velocities are distributed on average. The Boltzmann equation describes how collisions and external forces cause the velocity distribution to change. Through the Chapman-Enskog expansion of the Boltzmann equation, we can obtain the Euler, Navier-Stokes, Burnett equations, etc., according to the orders of approximation [1]. The lattice Boltzmann equation (LBE) is a discretized version of the Boltzmann equation in phase space and time [2–6]. Originally, the LBE was developed from the lattice-gas cellular automata [7–11], where fluids are simulated by using fictitious molecules hopping in regular lattices. The molecules collide with one another on the nodes of a lattice and move to other nodes successively. In the LBE, the fictitious molecules are replaced with a molecular probability distribution. There exist various models of the LBE according to the shape of lattice, the dimension of space, and the number of discrete velocities. Increasing the number of discrete velocities is a way to obtain models approaching the complete Galilean invariant [12] and the correct thermal results for compressible flows. However, the ratios of discrete velocities should be rational for collisions to occur on the nodes of regular lattices; otherwise additional effort is required. The models needing additional effort are called off-lattice models in contrast to on-lattice models having rational numbers for ratios of discrete velocities. Note that the models using the Gauss-type quadrature provide higher models, however, they are off-lattice models [13]. It is proposed to use the preservation of the norm and the orthogonality of the Hermite polynomial tensors for obtaining on-lattice models; however, with this framework it is difficult to obtain higher-order models because we should derive and calculate a system of equations for each model [14]. Using the minimization of an entropy function provides on-lattice models [15,16]; however, it has the same problem with the aforementioned framework.

In this paper, we derive a univariate polynomial equation whose variable is a discrete velocity. The coefficients of the equation are composed of the ratios between discrete velocities. Therefore, the problem to find an on-lattice model of any required level of accuracy is reduced to a problem only to solve the univariate polynomial equation. We also discuss the dependence of the stability of models on discretized equilibrium distributions. We present explicitly several on-lattice higher-order models to simulate the thermal shock tube problem with harsh conditions with respect to the previous LBE simulations. We compare the simulation results with the analytical solution of the Riemann problem [17] to illustrate the accuracy of our models. We also show the remarkable improvement of stability obtained by our models and our discretized equilibrium distributions.

The Boltzmann equation with the BGK collision term is $\partial_t f + \mathbf{V}\cdot\nabla f = -(f - f^{\mathrm{eq}})/\tau$. The infinitesimal quantity $f\,d\mathbf{x}d\mathbf{V}$ is the number of particles having velocity $\mathbf{V}$ in an infinitesimal element of phase space $d\mathbf{x}d\mathbf{V}$ at position $\mathbf{x}$ at time t. The relaxation time τ adjusts a tendency to approach the Maxwell-Boltzmann (MB) distribution f^{eq} due to collision. Macroscopic physical properties are obtained by $\rho\{1,\mathbf{U},e\} = \int f\{1,\mathbf{V},2^{-1}\|\mathbf{V}-\mathbf{U}\|^2\}d\mathbf{V}$ where ρ is number density, $\mathbf{U}$ macroscopic velocity, and e energy per unit of mass. We can relate e with temperature T by $e = Dk_BT/(2m_g)$ where D is the dimension of space, k_B the Boltzmann constant, and m_g molecular mass. The MB distribution is $f^{\mathrm{eq}} = \rho(\Theta_0\pi\theta)^{-D/2}\exp(-\|\mathbf{v}-\mathbf{u}\|^2/\theta)$ where dimensionless variables are defined by $\theta \equiv T/T_0$, $\mathbf{v} \equiv \Theta_0^{-1/2}\mathbf{V}$, and $\mathbf{u} \equiv \Theta_0^{-1/2}\mathbf{U}$ where $\Theta_0 \equiv 2k_BT_0/m_g$. The discretized version of the Boltzmann equation in phase space and time can be written by $f_i(\mathbf{x}+\mathbf{V}_i,t+\Delta t) - f_i(\mathbf{x},t) = -[f_i(\mathbf{x},t) - f_i^{\mathrm{eq}}(\mathbf{x},t)]/\tau$ where $f_i(\mathbf{x},t)$ is the probability for a particle to exist in a lattice site $\mathbf{x}$ at time t with discrete velocity $\mathbf{V}_i$. The essential work of the discretization is to find the discretized MB distribution f_i^{eq} including a set of discrete velocities.

II. UNIVARIATE POLYNOMIAL EQUATION

Here, we present a concise strategy to obtain f_i^{eq} and a set of discrete velocities. The discretized models can be accurate up to any required level and can be applied to regular lattices (on-lattice models). The lattice shapes are formed by line segment

*jae-wan.shim@polytechnique.org

for one-dimensional space, square for two-dimensional, cube for three-dimensional, etc. We find a model satisfying

$$\int \mathbf{v}^m f^{\mathrm{eq}}(\mathbf{v})\, d\mathbf{V} = \sum_i \mathbf{v}_i^m f_i^{\mathrm{eq}}(\mathbf{v}_i), \tag{1}$$

to conserve physical properties such as mass, momentum, pressure tensor, energy flux, and the change rate of the energy flux, etc., which are obtained by mth-order moments of $\mathbf{V}$, i.e., $\int \mathbf{V}^m f^{\mathrm{eq}}(\mathbf{V})d\mathbf{V}$. If we can express f^{eq} by a series expansion f_E^{eq} [18] having the form of

$$f^{\mathrm{eq}}(\mathbf{v}) \approx f_E^{\mathrm{eq}}(\mathbf{v}) = \exp(-v^2)P^{(N)}(\mathbf{v}), \tag{2}$$

where $P^{(N)}(\mathbf{v})$ is a polynomial of degree N in $\mathbf{v}$ and $v^2 = \mathbf{v}\cdot\mathbf{v}$, we can find f_i^{eq} in the form of

$$f_i^{\mathrm{eq}}(\mathbf{v}_i) = w_i P^{(N)}(\mathbf{v}_i), \tag{3}$$

where w_i are constant coefficients. We will show the method of obtaining f_E^{eq} with an example of the fifth order of the expression of f^{eq} by the multivariate Hermite series expansion [18] in this paper. By applying (2) and (3) to (1), we obtain

$$\int \exp(-v^2)P^{(m+N)}(\mathbf{v})\, d\mathbf{v} = \sum_i w_i P^{(m+N)}(\mathbf{v}_i). \tag{4}$$

We begin our systematic procedure with one-dimensional space. Formula (4) is satisfied for any polynomial of degree $m+N$, if and only if

$$\int v^n \exp(-v^2)\, dv = \sum_i w_i v_i^n, \tag{5}$$

for any non-negative integer $n \leqslant m+N$. It is easy to demonstrate this. Let us define $P^{(m+N)}(v) = \sum_{n=0}^{m+N} c_n v^n$. Then, Formula (4) becomes

$$\int \left\{ \exp(-v^2) \sum_{n=0}^{m+N} c_n v^n \right\} dv = \sum_i \left\{ w_i \sum_{n=0}^{m+N} c_n v_i^n \right\},$$

or

$$\sum_{n=0}^{m+N} c_n \left\{ \int \exp(-v^2) v^n\, dv - \sum_i w_i v_i^n \right\} = 0.$$

Therefore, for any coefficient c_n, Formula (4) is satisfied if Formula (5) is satisfied. And if Formula (5) is satisfied, we can construct any polynomial of degree $m+N$ by $P^{(m+N)}(v) = \sum_{n=0}^{m+N} c_n v^n$ where c_n is any desired coefficient. We can calculate the left side of (5) as

$$\int v^n \exp(-v^2)\, dv = \begin{cases} \Gamma\,[(n+1)/2] & \text{for } n = 2k \\ 0 & \text{for } n = 2k+1 \end{cases}, \tag{6}$$

where k is any non-negative integer and Γ is the Gaussian Gamma function which can be expressed by the double factorial as $\Gamma[(n+1)/2] = \sqrt{\pi}(n-1)!!/2^{n/2}$.

The system of equations (5) can become more concise by considering symmetry. We construct one-dimensional q-velocities models by defining the discrete velocities v_i and weight coefficients w_i as

$$\begin{aligned} &v_1 = 0, \quad v_{2i} > 0, \quad v_2 < v_4 < \cdots < v_{q-1}, \\ &v_{2i} = -v_{2i+1}, \text{ and } w_{2i} = w_{2i+1} > 0 \quad \text{for } i=1,2,\ldots,[q/2], \end{aligned} \tag{7}$$

where $[x]$ is the greatest integer that is less than or equal to x. Note that we regard q as an odd number to include the zero velocity v_1. To use regular lattices, the ratios of v_i should be rational numbers [19], therefore, we have the constraints of

$$v_{2(i+1)}/v_2 = p_{2(i+1)}/p_2 = \bar{p}_{2(i+1)} \quad \text{for } i = 1,2,\ldots,[q/2]-1, \tag{8}$$

where p_2 and $p_{2(i+1)}$ are relatively prime and $p_{2(i+1)} > p_{2i}$. These models have $2q$ variables composed of v_i and w_i, but have only q unknown variables by their symmetry (7). If p_2 and $p_{2(i+1)}$ are given, we can express all v_i by v_2. Consequently, we have $n' \equiv [q/2]+2 = (q+3)/2$ unknown variables which are v_2, w_1, and w_{2i} where $i = 1,2,\ldots,[q/2]$. The variables defined by (7) satisfy $\Xi(n) \equiv \sum w_i v_i^n = 0$ for any odd number n. Therefore, to find n' unknown variables, we need n' equations and they are

$$\{\Xi(n) = \Gamma[(n+1)/2] | n = 0,2,\ldots,2(n'-1)\}. \tag{9}$$

If the solution of (9) exists, it satisfies the polynomial of degree $m+N$ up to $2(n'-1)+1$ $(= q+2)$ in (4) because an odd number $2(n'-1)+1$ satisfies $\Xi(n) \equiv \sum w_i v_i^n = 0$ as was mentioned previously. Let us consider a q'-velocities model which does not possess the zero velocity, i.e., q' is an even number. It satisfies the polynomial up to $m+N = q'+1$. This implies a q-velocities model satisfies the same order of the moment accuracy $m+N$ as a $(q+1)$-velocities model where q is an odd number. Therefore, an odd number is preferred for the number of discrete velocities from the viewpoint of the minimization of discrete velocities.

The system of equations (9) can be reduced to a univariate polynomial equation. We define

$$\mathbf{w} = \begin{bmatrix} w_2 \\ w_4 \\ \vdots \\ w_{q-1} \end{bmatrix}, \quad \mathbf{A} = \begin{bmatrix} \bar{p}_2^2 & \bar{p}_4^2 & \cdots & \bar{p}_{q-1}^2 \\ \bar{p}_2^4 & \bar{p}_4^4 & \cdots & \bar{p}_{q-1}^4 \\ \vdots & \vdots & \ddots & \vdots \\ \bar{p}_2^{q-1} & \bar{p}_4^{q-1} & \cdots & \bar{p}_{q-1}^{q-1} \end{bmatrix},$$

$$\bar{\mathbf{p}}^n = \begin{bmatrix} \bar{p}_2^n \\ \bar{p}_4^n \\ \vdots \\ \bar{p}_{q-1}^n \end{bmatrix}^{\mathrm{T}}, \quad \text{and} \quad \Gamma = \frac{1}{2} \begin{bmatrix} \frac{1}{v_2^2}\Gamma\left(\frac{2+1}{2}\right) \\ \frac{1}{v_2^4}\Gamma\left(\frac{4+1}{2}\right) \\ \vdots \\ \frac{1}{v_2^{q-1}}\Gamma\left[\frac{(q-1)+1}{2}\right] \end{bmatrix},$$

where the superscript T is used for a transpose and $\bar{p}_2 = 1$. Then, Formula (9) is expressed by $\mathbf{A}\mathbf{w} = \Gamma$, $\bar{\mathbf{p}}^{q+1}\mathbf{w} = (2v_2^{q+1})^{-1}\Gamma\{[(q+1)+1]/2\}$, and $\sum_i w_i = \sqrt{\pi}$. If we eliminate $\mathbf{w}$ from the first two relations, we obtain a relation possessing only the variable v_2 with parameters $\bar{p}_{2(i+1)}$,

$$\bar{\mathbf{p}}^{q+1}\mathbf{A}^{-1}\Gamma = \left(2v_2^{q+1}\right)^{-1}\Gamma\left[\frac{(q+1)+1}{2}\right]. \tag{10}$$

Once we find the solution v_2 from (10), we can obtain the weight coefficients from $\mathbf{w} = \mathbf{A}^{-1}\Gamma$ and $w_1 = \sqrt{\pi} - \sum_{k=2}^{q} w_k$, and the discrete velocities from (8). Note that the solution of weight coefficients can have imaginary or real negative values, which are excluded for the positivity of weight coefficients.

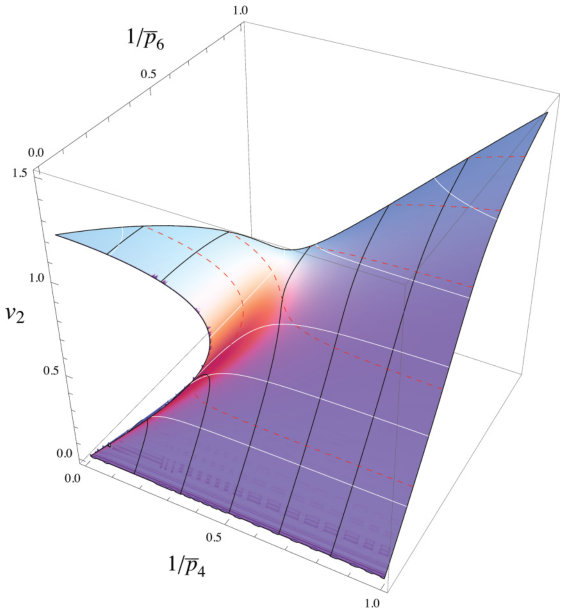

FIG. 1. (Color online) Three-dimensional plot generated by Eq. (10) when $q = 7$.

We plot Formula (10) for the 7-velocities model in Fig. 1. We will compare a part of this figure with the solution of the 5-velocities model in this paper. We have obtained the discrete velocities and the weight coefficients of one-dimensional models. Therefore, we can easily construct higher-dimensional models from the one-dimensional ones according to tensor products of one-dimensional velocities [15]. To reduce the number of discrete velocities for hypercubic [20] multidimensional cases, we have obtained uniform polynomial equations,

$$\sum_i w_i \mathbf{v}_i^n = \prod_{\alpha=1}^{D} \Gamma\left[(a_\alpha+1)/2\right] \text{ for } n = 0,2,4,\ldots,n_{\max} \leqslant m + k \text{ and even } a_\alpha,$$

where m is the maximum order of moment satisfied in (1) and k is the degree of polynomial such as the degree of Taylor expansion (TE) or Hermite expansion (HE) of the equilibrium distribution and $\mathbf{v}_i^n \equiv v_{i,x_1}^{a_1} v_{i,x_2}^{a_2} \cdots v_{i,x_D}^{a_D}$ such that $a_1 + a_2 + \cdots + a_D = n$ and $a_\alpha \in \mathbb{N}_0$ for $\alpha = 1,2,\ldots,D$. The subscripts x_i for $i = 1,2,\ldots,D$ signify the coordinates in a D-dimensional Cartesian coordinate system. The solutions of the uniform polynomial equations include the well-known lower-order models. All solutions of the uniform polynomial equations satisfy the rotational invariance by a selection of a set of discrete velocities having rotational invariance. The detail of multidimensional cases will be studied elsewhere.

III. DISCRETIZED EQUILIBRIUM DISTRIBUTION

From now on, we find f_E^{eq} of Formula (2) to prepare discretized equilibrium distributions. For any multidimensional variable $\mathbf{x}$, the Nth-order Taylor expansion of a function g about $\mathbf{x} = \mathbf{x}_0$ is

$$g^{(N)}(\mathbf{x}) = \sum_{n=0}^{N} \frac{1}{n!}\left[\left((\mathbf{x}-\mathbf{x}_0)\cdot\frac{\partial}{\partial \mathbf{x}'}\right)^n g(\mathbf{x}')\right]_{\mathbf{x}'=\mathbf{x}_0}. \quad (11)$$

We define a $D+1$-dimensional variable $\mathbf{y}$ by combining the D-dimensional macroscopic velocity $\mathbf{u}$ and the temperature θ as $\mathbf{y} = (\mathbf{u},\theta)$. The Nth-order Taylor expansion (TE) $f_{\text{TE}}^{\text{eq}\ (N)}$ of the MB distribution about $\mathbf{y}_0 = (\mathbf{0},\theta_0)$ can be written as $f_{\text{TE}}^{\text{eq}\ (N)}(\mathbf{y}) = g^{(N)}(\mathbf{y})$. We assume that $\mathbf{u}$ and θ are infinitely small quantities of the same order in this expansion. If we assume $\mathbf{u}$ and $\theta^{1/2}$ are the same order, we obtain another TE $f_{\text{HE}}^{\text{eq}\ (N)}(\mathbf{z}) = g^{(N)}(\mathbf{z})$ about $\mathbf{z}_0 = (\mathbf{0},0)$ by defining $\mathbf{z} = (\mathbf{u},\sigma)$ where $\varepsilon\sigma^2 = \theta - 1$ and $\varepsilon = \pm 1$. This is identical to the Hermite expansion (HE) of order N [18]. For example, the fifth order of the expression of f^{eq} by the multivariate Hermite series expansion is given by

$$f(\mathbf{v},\mathbf{u},\theta) = (\Theta_0\pi)^{-D/2}\exp(-v^2)\sum_{n=0}^{5}\frac{1}{n!}\mathbf{a}^{(n)}\cdot\mathbf{H}^{(n)},$$

where

$$\begin{aligned}
\mathbf{a}^{(0)}\cdot\mathbf{H}^{(0)} &= 1,\\
\mathbf{a}^{(1)}\cdot\mathbf{H}^{(1)} &= \bar{\mathbf{u}}\cdot\bar{\mathbf{v}},\\
\mathbf{a}^{(2)}\cdot\mathbf{H}^{(2)} &= (\bar{\mathbf{u}}\cdot\bar{\mathbf{v}})^2 + (\theta-1)(\bar{v}^2 - D) - \bar{u}^2,\\
\mathbf{a}^{(3)}\cdot\mathbf{H}^{(3)} &= (\bar{\mathbf{u}}\cdot\bar{\mathbf{v}})[(\bar{\mathbf{u}}\cdot\bar{\mathbf{v}})^2 - 3\bar{u}^2 + 3(\theta-1)(-2-D+\bar{v}^2)],\\
\mathbf{a}^{(4)}\cdot\mathbf{H}^{(4)} &= (\bar{\mathbf{u}}\cdot\bar{\mathbf{v}})^4 - 6(\bar{\mathbf{u}}\cdot\bar{\mathbf{v}})^2\bar{u}^2 + 3\bar{u}^4\\
&\quad + 6(\theta-1)\{(\bar{\mathbf{u}}\cdot\bar{\mathbf{v}})^2[\bar{v}^2 - (D+4)]\\
&\quad + (D+2-\bar{v}^2)\bar{u}^2\} + 3(\theta-1)^2\\
&\quad \times[\bar{v}^4 - 2(D+2)\bar{v}^2 + D(D+2)],
\end{aligned}$$

and

$$\begin{aligned}
\mathbf{a}^{(5)}\cdot\mathbf{H}^{(5)} &= (\bar{\mathbf{u}}\cdot\bar{\mathbf{v}})[(\bar{\mathbf{u}}\cdot\bar{\mathbf{v}})^4 - 10(\bar{\mathbf{u}}\cdot\bar{\mathbf{v}})^2\bar{u}^2 + 15\bar{u}^4]\\
&\quad + 10(\theta-1)(\bar{\mathbf{u}}\cdot\bar{\mathbf{v}})[\bar{v}^2(\bar{\mathbf{u}}\cdot\bar{\mathbf{v}})^2 - (D+6)(\bar{\mathbf{u}}\cdot\bar{\mathbf{v}})^2\\
&\quad - 3\bar{u}^2\bar{v}^2 + 3(D+4)\bar{u}^2] + 15(\theta-1)^2(\bar{\mathbf{u}}\cdot\bar{\mathbf{v}})\\
&\quad \times[\bar{v}^4 - 2(D+4)\bar{v}^2 + (D^2+6D+8)].
\end{aligned}$$

where $\bar{\mathbf{u}} = \sqrt{2}\mathbf{u}$ and $\bar{\mathbf{v}} = \sqrt{2}\mathbf{v}$ [18]. The expansions $f_{\text{TE}}^{\text{eq}\ (N)}$ and $f_{\text{HE}}^{\text{eq}\ (N)}$ satisfy

$$\int \mathbf{v}^m f^{\text{eq}}(\mathbf{v})\,d\mathbf{v} = \int \mathbf{v}^m f_E^{\text{eq}}(\mathbf{v})\,d\mathbf{v}, \quad (12)$$

for $0 \leqslant m \leqslant N$. This is clear if we regard $f^{\text{eq}}(\mathbf{v})$ as an infinite series expansion in $\mathbf{u}$ and θ. The evaluated result of the left-hand side, $\int \mathbf{v}^m f^{\text{eq}}(\mathbf{v})\,d\mathbf{v}$, contains the terms $\mathbf{u}^\alpha\theta^\beta$ where $\alpha + 2\beta = m$ for α and β being non-negative integers. Therefore, if we include the terms $\mathbf{u}^\alpha\theta^\beta$ in the series expansions $f_{\text{TE}}^{\text{eq}\ (N)}$ and $f_{\text{HE}}^{\text{eq}\ (N)}$, Formula (12) is satisfied. Note that $f_{\text{HE}}^{\text{eq}\ (N)}$ itself is a polynomial of degree N of $\mathbf{v}$; however, $f_{\text{TE}}^{\text{eq}\ (N)}(\mathbf{v})$ is of degree $2N$ appearing in $\partial^N f^{\text{eq}}/\partial\theta^N|_{\theta=\theta_0}$.

IV. ORDER OF ACCURACY

Consequently, if we use the one-dimensional q-velocities models obtained by (9) with $f_{\text{TE}}^{\text{eq}\ (N)}$, it is guaranteed that the moments evaluated from f_i^{eq} are identical to those from f^{eq} up to the mth-order where $m \leqslant \min[N,\ q+2-2N]$. The reason is that $f_{\text{TE}}^{\text{eq}\ (N)}$ satisfies (12) for $m \leqslant N$ and the q-velocities model satisfies $\Xi(q+2) = 0$ under the condition that $f_{\text{TE}}^{\text{eq}\ (N)}$ itself is a polynomial of degree $2N$. Similarly, if we use $f_{\text{HE}}^{\text{eq}\ (N)}$, we have the condition of satisfaction, $m \leqslant \min[N,\ q+2-N]$. Therefore, we can obtain sufficiently accurate models of the thermal lattice Boltzmann equation by controlling q and N. The use of $f_{\mathrm{HE}}^{\mathrm{eq}\,(N)}$ between TE and HE is optimal to reduce the number of discrete velocities in a given level of accuracy. However, from the viewpoint of stability, $f_{\mathrm{TE}}^{\mathrm{eq}\,(N)}$ performs better with respect to $f_{\mathrm{HE}}^{\mathrm{eq}\,(N)}$. It seems the higher-order terms in θ appearing in $f_{\mathrm{TE}}^{\mathrm{eq}\,(N)}$ stabilize the models of the LBE because it is the only difference between $f_{\mathrm{TE}}^{\mathrm{eq}\,(N)}$ and $f_{\mathrm{HE}}^{\mathrm{eq}\,(N)}$. We will demonstrate it at the simulation part of this paper. Note that the discretized equilibrium distribution is $f_i^{\mathrm{eq}} = \rho w_i P(v_i)$ where $P(v) = \theta^{1/2}\exp(v^2) f_E^{\mathrm{eq}}(v)$ and f_E^{eq} is $f_{\mathrm{TE}}^{\mathrm{eq}}$ or $f_{\mathrm{HE}}^{\mathrm{eq}}$.

V. MODEL EXAMPLES

We explicitly present some models. We will give only the values of v_2 and $\bar{w}_{2i}$ because the others are easy to obtain by (7) and $\bar{w}_1 = 1 - \sum_{k=2}^{q}\bar{w}_k$. When $q = 3$, we obtain the well-known solution of $v_2 = \sqrt{3/2}$ and $\bar{w}_2 = 1/6$ where $\bar{w}_i = w_i/\sqrt{\pi}$. When $q = 5$, we obtain

$$\begin{aligned} v_2 &= (3 + 3r^2 \pm \chi)^{1/2}/2, \\ \bar{w}_2 &= [9r^4 - 27r^2 - 6 \mp (3r^2 - 2)\chi]/[300r^2(r^2 - 1)], \\ \bar{w}_4 &= [6r^4 + 27r^2 - 9 \mp (2r^2 - 3)\chi]/[300(r^2 - 1)], \end{aligned} \tag{13}$$

where $\chi = (9r^4 - 42r^2 + 9)^{1/2}$ and $r = 1/\bar{p}_4$. The weight coefficients $\bar{w}_i$ are the same as those from the entropic method [15,16]; however, instead of their fixed reference temperature for isothermal models, we provide the speeds of the discrete velocities for thermal models. Note that the first relation describing v_2 in (13) can be found as a graph in Fig. 1 when $\bar{p}_6$ approaches infinity.

We define a ghost velocity by v_i whose weight coefficient $\bar{w}_i$ is very small. For example, we can have a q-velocities model having a pair of ghost velocities v_{q-1} and v_q. When $\bar{w}_q$ approaches zero, the solution of (9) for a q-velocities model satisfies $\Xi(q+1) = \Gamma(q+2/3)$ in addition to the system of equations for a $(q-2)$-velocities model. Consequently, the solution for a q-velocities model having a pair of ghost velocities approaches the solution for a $(q-2)$-velocities model with giving us additional information of $\bar{w}_q$ and v_q. This exactly occurs in the 5-velocities model (13) drawn in Fig. 2. When r approaches zero, the solution represented by dashed lines approaches that of the 3-velocities model, and the solution of the 7-velocities model in Fig. 1 approaches that of the 5-velocities model when $1/p_6$ approaches zero. Therefore, it is better to use a solution set without ghost velocities to avoid the downgrade of the number of discrete velocities. We show the stability issue related to the ghost velocities.

VI. SIMULATION EXAMPLES

A one-dimensional shock tube (linear 1000 nodes) simulation was performed by the two solutions of the 5-velocities model (13) with $r = 1/3$ and $f_{\mathrm{HE}}^{\mathrm{eq}\,(2)}$. The initial condition is a density step $C_L = \{\rho = p = 3,\ \theta = 1,\ u = 0\}$ for $X < 500$ and $C_R = \{\rho = p = \theta = 1,\ u = 0\}$ for $X \geqslant 500$. The boundary condition is C_L at $X = 1$ and C_R at $X = 1000$. The relaxation time is $\tau = 1$. We observe the fluctuation only in the case of the solution having ghost velocities in Fig. 3. For the next simulation, we will use the stable solution.

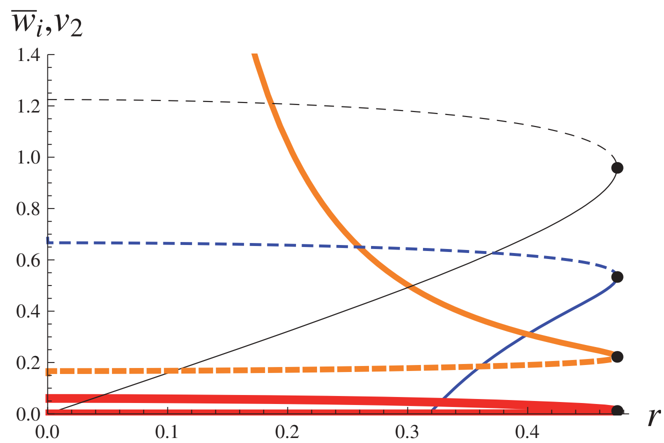

FIG. 2. (Color online) The graph of Eq. (13) is drawn. Two families are plotted and distinguished by dashed and solid lines. The thinner black line is for v_2, the thin blue for $\bar{w}_1$, the medium orange for $\bar{w}_2$, the thicker red for $\bar{w}_4$. The black dots indicate $\bar{w}_i$ and v_2 merged into identical values.

The shock tube problem was simulated by the 5-, 7-, and 11-velocities models with the ratios of discrete velocities and the base discrete velocity $(\bar{p}_4, v_2) = (3, 0.553\,432)$, $(\bar{p}_4, \bar{p}_6, v_2) = (2, 3, 0.846\,393)$, and $(\bar{p}_4, \bar{p}_6, \bar{p}_8, \bar{p}_{10}, v_2) = (2, 3, 4, 5, 0.685\,900)$, respectively. We can easily calculate the weight coefficients by $\mathbf{w} = \mathbf{A}^{-1}\Gamma$. Because of the page limit, we give only the values of v_2 and $\bar{p}_{2i}$. The boundary and initial conditions and the geometry are the same for the simulation of Fig. 3. The simulation results are in excellent agreement with the analytical solution of the Riemann problem except the result obtained by the 5-velocities model with $f_{\mathrm{TE}}^{\mathrm{eq}\,(2)}$ having the second-order moment accuracy. For the physical properties ρ, p, θ, and u, the subscripts 1 and 2 will be used to indicate that the values are extracted from the positions $X = 430$ and 650, respectively, where the plateaus appear. When $(q, N, m) = (5, 3^*, 3)$, $(7, 3, 3)$, and $(11, 4, 4)$, the results are $\rho_1 = 2.46$, $\rho_2 = 1.18$, $p_{1,2} = 1.65$, $\theta_1 = 0.67$, $\theta_2 = 1.40$, and $u_{1,2} = 0.22$ as in the solution of the Riemann problem. When $(q, N, m) = (5, 2, 2)$, the results are $\rho_1 = 2.43$,

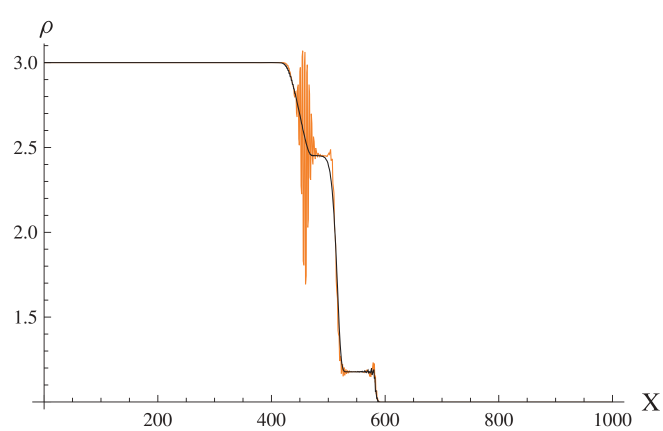

FIG. 3. (Color online) Simulation of shock tube obtained by the 5-velocities models. The black and orange (gray) lines are the results from the solutions of the dashed and the solid lines of Fig. 2, respectively.

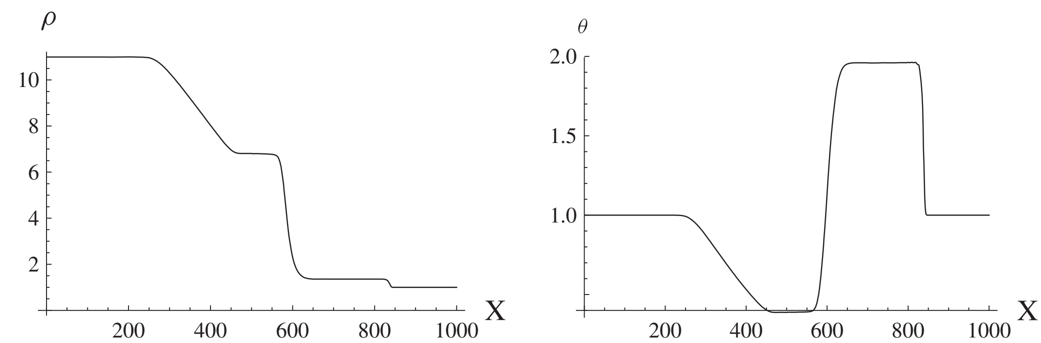

FIG. 4. Simulation of the one-dimensional (1000 nodes) shock tube problem by the 21-velocities model with $f_{\mathrm{TE}}^{\mathrm{eq}\ (5)}$ and the relaxation time $\tau = 1$.

$\rho_2 = 1.18$, $p_{1,2} = 1.64$, $\theta_1 = 0.68$, $\theta_2 = 1.39$, $u_1 = 0.23$, and $u_2 = 0.22$. Note that N is the order of the TE ($N = 2,3,4$) and HE ($N = 3^*$); m is the maximum order of the satisfied moment; q is the number of discrete velocities.

If we pass a critical value of the density ratio between the left ($X < 500$) and the right ($X \geqslant 500$) domains in the initial and boundary conditions of the shock tube problem, the models of the LBE become unstable. Also, the decrease of the viscosity below a critical value by decreasing the relaxation time τ makes the models unstable. By virtue of (10), we could find the models having a high number of discrete velocities to obtain robustness. Moreover, we realized that $f_{\mathrm{HE}}^{\mathrm{eq}\ (N)}$ is not optimal from the viewpoint of stability. The following simulation shows the robustness of our 21-velocities model $(\bar{p}_4, \bar{p}_6, \bar{p}_8, \bar{p}_{10}, \bar{p}_{12}, \bar{p}_{14}, \bar{p}_{16}, \bar{p}_{18}, \bar{p}_{20}, v_2) = (2,3,4,5,6,7,8,9,11,0.372\,889)$ and our discretized equilibrium distribution $f_{\mathrm{TE}}^{\mathrm{eq}\ (5)}$. Under the initial condition $\bar{C}_L = \{\rho = p = 11,\ \theta = 1,\ u = 0\}$ for $X < 500$ and $C_R = \{\rho = p = \theta = 1,\ u = 0\}$ for $X \geqslant 500$ and the boundary condition $\bar{C}_L$ at $X = 1$ and C_R at $X = 1000$, the simulation was stable with $\tau = 1$ as in Fig. 4, although the density ratio was 11. However, $f_{\mathrm{HE}}^{\mathrm{eq}\ (N)}$ with $N \leqslant 10$ could not pass the simulation test with the same conditions. Note that $f_{\mathrm{HE}}^{\mathrm{eq}\ (10)}$ includes all terms appearing in $f_{\mathrm{TE}}^{\mathrm{eq}\ (5)}$.

VII. CONCLUSION

In conclusion, we have derived a univariate polynomial equation providing on-lattice higher-order models of the thermal LBE. Finding an on-lattice model of any required level of accuracy is reduced to only solving the univariate polynomial equation. This opens a way to construct the robust models having high number of discrete velocities. Moreover, we have presented discretized equilibrium distributions which are more robust than those obtained from the HE.

ACKNOWLEDGMENTS

This research was partially supported by the KIST Institutional Program and by the WCI Program of the National Research Foundation of Korea funded by the Ministry of Education, Science and Technology of Korea (NRF Grant No. WCI 2009-003).

[1] C. Cercignani, *Mathematical Methods in Kinetic Theory* (Plenum, New York, 1990).
[2] X. He and L.-S. Luo, Phys. Rev. E **56**, 6811 (1997).
[3] T. Abe, J. Comput. Phys. **131**, 241 (1997).
[4] X. Shan and X. He, Phys. Rev. Lett. **80**, 65 (1998).
[5] S. Ansumali, I. V. Karlin, and H. C. Öttinger, Europhys. Lett. **63**, 798 (2003).
[6] X. Shan, X.-F. Yuan, and H. Chen, J. Fluid Mech. **550**, 413 (2006).
[7] U. Frisch, B. Hasslacher, and Y. Pomeau, Phys. Rev. Lett. **56**, 1505 (1986).
[8] F. J. Higuera, S. Succi, and R. Benzi, Europhys. Lett. **9**, 345 (1989).
[9] J. W. Shim and R. Gatignol, Phys. Rev. E **81**, 046703 (2010).
[10] Y. H. Qian, D. D'Humières, and P. Lallemand, Europhys. Lett. **17**, 479 (1992).
[11] H. Chen, S. Chen, and W. H. Matthaeus, Phys. Rev. A **45**, R5339 (1992).
[12] Y. H. Qian and Y. Zhou, Europhys. Lett. **42**, 359 (1998).
[13] W. P. Yudistiawan, S. K. Kwak, D. V. Patil, and S. Ansumali, Phys. Rev. E **82**, 046701 (2010).
[14] P. C. Philippi, L. A. Hegele, L. O. E. dosSantos, and R. Surmas, Phys. Rev. E **73**, 056702 (2006).
[15] S. S. Chikatamarla and I. V. Karlin, Phys. Rev. Lett. **97**, 190601 (2006).
[16] S. S. Chikatamarla and I. V. Karlin, Phys. Rev. E **79**, 046701 (2009).
[17] R. Courant and K. O. Friedrichs, *Supersonic Flow and Shock Waves* (Springer-Verlag, New York, 1976), p. 181.
[18] J. W. Shim and R. Gatignol, Z. Angew. Math. Phys. (2012), doi: 10.1007/s00033-012-0265-1.
[19] J. W. Shim and R. Gatignol, Phys. Rev. E **83**, 046710 (2011).
[20] H. S. M. Coxeter, *Regular Polytopes* (Dover, New York, 1973), p. 123.